

## BIOCATALYSIS

# Design of an in vitro biocatalytic cascade for the manufacture of islatravir

Mark A. Huffman<sup>1\*</sup>, Anna Fryszkowska<sup>1\*</sup>, Oscar Alvizo<sup>2</sup>, Margie Borra-Garske<sup>2</sup>, Kevin R. Campos<sup>1</sup>, Keith A. Canada<sup>1</sup>, Paul N. Devine<sup>1</sup>, Da Duan<sup>2</sup>, Jacob H. Forstater<sup>1</sup>, Shane T. Grosser<sup>1</sup>, Holst M. Halsey<sup>1</sup>, Gregory J. Hughes<sup>1</sup>, Junyong Jo<sup>1</sup>, Leo A. Joyce<sup>1†</sup>, Joshua N. Kolev<sup>1</sup>, Jack Liang<sup>2</sup>, Kevin M. Maloney<sup>1</sup>, Benjamin F. Mann<sup>1</sup>, Nicholas M. Marshall<sup>1‡</sup>, Mark McLaughlin<sup>1</sup>, Jeffrey C. Moore<sup>1</sup>, Grant S. Murphy<sup>1</sup>, Christopher C. Nawrat<sup>1</sup>, Jovana Nator<sup>2</sup>, Scott Novick<sup>2</sup>, Niki R. Patel<sup>1</sup>, Agustina Rodriguez-Granillo<sup>3§</sup>, Sandra A. Robaire<sup>1</sup>, Edward C. Sherer<sup>3</sup>, Matthew D. Truppo<sup>1¶</sup>, Aaron M. Whittaker<sup>1</sup>, Deeptak Verma<sup>3</sup>, Li Xiao<sup>3</sup>, Yingju Xu<sup>1</sup>, Hao Yang<sup>1</sup>

Enzyme-catalyzed reactions have begun to transform pharmaceutical manufacturing, offering levels of selectivity and tunability that can dramatically improve chemical synthesis. Combining enzymatic reactions into multistep biocatalytic cascades brings additional benefits. Cascades avoid the waste generated by purification of intermediates. They also allow reactions to be linked together to overcome an unfavorable equilibrium or avoid the accumulation of unstable or inhibitory intermediates. We report an in vitro biocatalytic cascade synthesis of the investigational HIV treatment islatravir. Five enzymes were engineered through directed evolution to act on non-natural substrates. These were combined with four auxiliary enzymes to construct islatravir from simple building blocks in a three-step biocatalytic cascade. The overall synthesis requires fewer than half the number of steps of the previously reported routes.

The structural complexity of new drug molecules and the growing desire to develop green and efficient synthetic processes demand innovation and excellence in organic chemistry (1). Enzyme catalysis incorporated into pharmaceutical manufacturing represents one such innovation, providing benefits that include unparalleled selectivity, increased atom economy, and improved safety (2, 3). But a truly transformative potential lies in combining two or more enzymatic steps into biocatalytic cascade sequences (4, 5). Biocatalytic cascades save resources by avoiding isolation of intermediates. They also allow thermodynamically unfavorable steps to be coupled to more favorable reactions and can avoid enzyme inhibition by consuming inhibitory intermediates as they are formed. Cascades are enabled by the exceptional chemoselectivity of enzymes and their compatibility with a common set of mild aqueous reaction conditions. Designing chemical syntheses around the use of multienzyme cascades could revolutionize the manufacture of drugs. Putting this vision into practice requires a capacity for rapid identification and

engineering of multiple enzymes to act on unnatural substrates at industrially relevant concentrations. Ongoing advances in directed evolution (6, 7), combined with an increasing abundance of genomic information, have now brought this goal within reach, enabling us to construct a nine-enzyme cascade to manufacture the investigational HIV treatment islatravir.

The nucleoside analog islatravir (MK-8591, EFdA, 1) is an HIV reverse transcriptase translocation inhibitor with a previously undeveloped mechanism of action (8, 9). Its extraordinary potency and long duration of action promise utility in reduced-frequency dosing regimens for HIV treatment and preexposure prophylaxis (10). Several synthetic routes to islatravir have been published, each requiring between 12 and 18 steps (11–15). Inefficiencies in the previous syntheses arose from the need for multiple protecting-group manipulations as well as the difficulty of controlling anomeric stereochemistry in 2'-deoxyribonucleosides. Enzymatic reactions often eliminate the need for protecting groups while at the same time providing precise control over stereoselectivity. We therefore envisaged that biocatalysis might effectively address the synthetic challenges of islatravir.

The bacterial nucleoside salvage pathway (Fig. 1A) provides an attractive biocatalytic retrosynthetic scheme for deoxyribonucleosides (16, 17). The biological sequence degrades purine 2'-deoxyribonucleosides using three enzymes (18). First, purine nucleoside phosphorylase (PNP) displaces the nucleobase with phosphate to give deoxyribose 1-phosphate. Phosphopentomutase (PPM) then transfers

the phosphate to the 5 position. The resulting sugar 5-phosphate becomes a substrate for deoxyribose 5-phosphate aldolase (DERA), which performs a retro-aldol cleavage into glyceraldehyde 3-phosphate and acetaldehyde. This sequence can rapidly assemble nucleosides from simple starting materials when run in reverse (17). Using the salvage pathway to synthesize islatravir requires all three enzymes to act on non-natural substrates bearing a fully substituted carbon at C-4 of the 2-deoxyribose ring. The full sequence of enzymes has not been used to both construct a non-natural sugar and attach a nucleobase. Nonetheless, we were encouraged by previous applications of PNP and PPM to produce non-natural nucleosides (17, 19) as well as the ability of DERA to make non-natural sugars (20).

The reversibility of the reactions in the salvage pathway allowed us to rapidly explore the sequence in the retrosynthetic direction (19), starting from islatravir. We began by evaluating a panel of purine phosphorylases for their ability to cleave islatravir into the nucleobase (2) and sugar 1-phosphate (3). The ethynyl substituent was accepted by several homologs, with the native *Escherichia coli* PNP showing the highest activity. Application of the *E. coli* enzyme at high loading generated the otherwise inaccessible 1-phosphate intermediate (3) to use in testing phosphopentomutases. The native *E. coli* PPM displayed the highest activity for converting this unnatural substrate to the thermodynamically favored 5-phosphate (4). With compelling proof of concept for the two desired reactions in place, we then focused on improving the activity of both enzymes by means of directed evolution.

We used a homology model based on the *Bacillus cereus* PPM crystal structure to generate a library of variants with single mutations near the active site, which were screened for improved activity in the reverse reaction. In the best performing variant, the manganese-binding D172 was replaced by a noncoordinating alanine (fig. S1D). Recombination of beneficial mutations from the first round—including a change in the catalytic, phosphorous-transferring residue T97S—resulted in a quintuple mutant that exhibited  $\geq 70$ -fold improvement over the wild-type enzyme (Table 1 and figs. S22 to S24). (Single-letter abbreviations for the amino acid residues are as follows: A, Ala; C, Cys; D, Asp; E, Glu; F, Phe; G, Gly; H, His; I, Ile; K, Lys; L, Leu; M, Met; N, Asn; P, Pro; Q, Gln; R, Arg; S, Ser; T, Thr; V, Val; W, Trp; and Y, Tyr. In the mutants, other amino acids were substituted at certain locations; for example, T97S indicates that threonine at position 97 was replaced by serine.)

The improved PPM variant enabled us to evolve PNP for improved activity. We screened a library of variants with single mutations near the active site for formation of islatravir in

<sup>1</sup>Process Research and Development, Merck & Co., Inc., Rahway, NJ 07065, USA. <sup>2</sup>Codexis, Inc., 200 Penobscot Drive, Redwood City, CA 94063, USA. <sup>3</sup>Computational and Structural Chemistry, Discovery Chemistry, Merck & Co., Inc., Kenilworth, NJ 07033, USA.

\*Corresponding author. Email: mark\_huffman@merck.com (M.A.H.); anna.fryszkowska@merck.com (A.F.) †Present address: Arrowhead Pharmaceuticals, 502 South Rosa Road, Madison, WI 53719, USA. ‡Present address: Invenra, 505 South Rosa Road, Madison, WI 53719, USA. §Present address: Schrodinger, 222 Third St, Cambridge, MA 02142, USA. ¶Present address: Janssen Research & Development, Spring House, PA 19477, USA.

the tandem forward reaction from sugar 5-phosphate (**4**), with the 1-phosphate (**3**) being generated in situ by the newly evolved PPM. A single amino acid change, M64A, near the alkyne-bearing C-4 of the docked substrate (fig. S1E) provided a PNP variant with about 350-fold improved activity (Table 1 and figs. S26 and S27). With the two active enzymes, we focused our attention on evaluating the practicality of the glycosylation cascade.

Because the PPM-catalyzed equilibrium favors the starting 5-phosphate, the phosphate transfer and glycosylation reactions must be performed simultaneously. Despite the improved activity of both enzymes, the tandem reaction plateaued at <50% yield. A reverse reaction starting from islatravir reached 40% conversion, demonstrating that the reaction was equilibrium limited. In addition, the inorganic phosphate byproduct of the glycosylation reaction is known to inhibit PPM (*21*). Removing the inorganic phosphate as it is formed provided an effective solution to the equilibrium and inhibition problems (*22*). Addition of sucrose phosphorylase (SP) and sucrose to the reaction converts free phosphate to glucose 1-phosphate and shifts the entire equilibrium forward. The resulting three-enzyme cascade runs to full conversion at substrate concentrations as high as 200 mM (scheme S4B).

We continued exploring the retrosynthetic degradation pathway by screening DERA en-

zymes in the retro-aldol reaction. Several DERA homologs displayed high activity in the retro-aldol of the alkynylated sugar. After further evaluation in the forward aldol reaction, we selected the DERA from *Shewanella halifaxensis* for its high activity, complete stereoselectivity in the formation of the new C-C bond (> 99% de), and kinetic selectivity favoring reaction with the (*R*)-enantiomer of the aldehyde. The (*S*)-aldehyde was very slowly converted to the (*3S,4S*) diastereomer. This wild-type DERA was also active in reaction with the nonphosphorylated aldehyde (**7**). Despite extensive research on applications of DERA enzymes, we did not find any reports of reactions of aldehydes with a fully substituted  $\alpha$ -carbon.

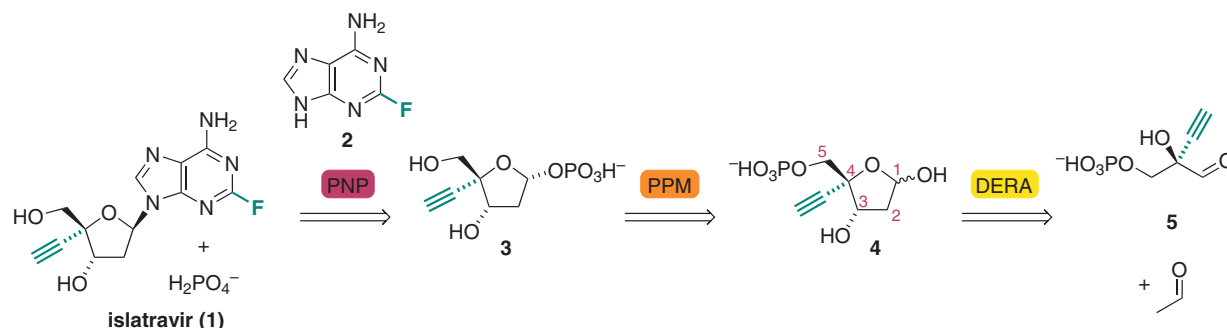
The limitation of the *S. halifaxensis* DERA was that it did not tolerate the high concentrations of acetaldehyde required for a practical synthesis. Two rounds of directed evolution addressed this constraint, yielding an improved variant that retained high activity at an acetaldehyde concentration >400 mM (Table 1). The engineered enzyme contained several new mutations, including C47V (fig. S1C). This cysteine residue is found near the active site in other DERA homologs and acts as a regulator of the enzyme activity, binding the product of acetaldehyde self-aldol condensation (*23*).

With the repurposed nucleoside salvage enzymes in hand, we focused on an efficient synthesis of 2-ethynylglyceraldehyde 3-phosphate

(**5**). Known biochemical pathways to its natural analog (*R*)-glyceraldehyde phosphate do not allow for facile incorporation of a C-2-substituent. Retrosynthetic analysis suggested that **5** could be accessed from the simple achiral building block 2-ethynylglycerol (**6**) through oxidation and phosphorylation reactions (Fig. 1B). In theory, these transformations could occur in either order. We explored enzymes for all four of these reactions and did not find any with activity for oxidation of **8**. We therefore pursued the path of oxidation followed by phosphorylation.

Discovery of an enzyme with phosphorylation activity toward **7** required extensive screening of a broad spectrum of kinases that naturally act on sugars and primary alcohols. Ultimately, we identified a pantothenate kinase (PanK) from *E. coli* with very low-level activity toward the (*R*)-enantiomer of aldehyde **7**. Applying directed evolution, we were able to rapidly increase the activity by introducing two mutations (L277I and I281M) in the helix of the pantothenate binding site (fig. S1B). Further engineering improved the enzyme's activity and stability. The evolved variant displayed greater than 100-fold higher activity (fig. S19) and pro-(*R*) kinetic selectivity (*E* = 8) (scheme S19), achieving full conversion at 200 mM concentration (Table 1). Practical use of the kinase in vitro required regeneration of its cofactor adenosine triphosphate. We chose

### A Bacterial nucleoside salvage pathway applied to islatravir (**1**). Unnatural structural elements are highlighted in green.



### B Biocatalytic retrosynthetic analysis of aldehyde intermediate (**5**).

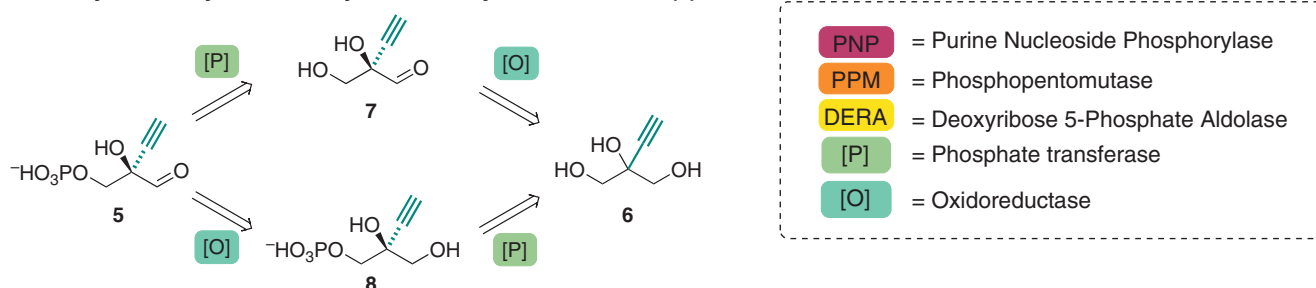


**Fig. 1. Biocatalytic retrosynthetic planning.** (A) Purine nucleoside degradation pathway applied retrosynthetically to islatravir (**1**). (B) Retrosynthesis of the glyceraldehyde phosphate analog leading to a simple achiral building block.

acetyl phosphate as an economical source of activated phosphate paired with a thermostable acetate kinase (AcK) from *Thermotoga maritima* (Fig. 2).

The final piece to complete the biocatalytic pathway was the desymmetrizing oxidation of 2-ethynylglycerol (**6**). Among a broad range of oxidoreductases, we identified evolved variants of galactose oxidase (GOase M1 and F2) that chemoselectively formed the monoaldehyde **7** with limited overoxidation (Table 1). These copper-dependent enzymes were previously engineered for improved expression in *E. coli* (M1-variant) (24) and broadened substrate scope (F2-variant) (25). Unfortunately, both M1 and F2 GOase variants favored formation of the undesired (*S*)-enantiomer with 8:92 and 40:60 *R:S* ratios, respectively. The (*S*)-selectivity is consistent with the stereochemistry of the natural substrate D-galactose. Nevertheless, the relaxed stereoselectivity of the F2-variant suggested that its enantioselectivity could be reversed, and the GOase F2 became the starting point for evolution.

Synthetic applications of GOases require two additional redox enzymes: a catalase to disproportionate the hydrogen peroxide byproduct and a peroxidase to maintain the correct oxidation state of copper (26). We chose commercially available bovine catalase and horseradish peroxidase and used these enzymes during evolution of the GOase. Over 12 rounds of oxidase engineering, we targeted an improvement in activity, a reduction in product inhibition, and a reversal of the innate enantioselectivity. The engineered oxidase displayed 11-fold improved activity and a reversed 90:10 *R:S* selectivity (Table 1). The change in enantioselectivity resulted mainly from two mutations in the active site: W290Y

and F464L (fig. S1A). Multiple additional mutations throughout the enzyme improved protein expression, stability, and activity and alleviated product inhibition. With higher activity came an increase in overoxidation of the product. The overoxidation led to an increase in the enantiopurity of **7** throughout the course of the reaction (up to 99% enantiomeric excess), albeit at the cost of yield (fig. S10).

At this point, we had evolved enzymes for each step of a fully biocatalytic sequence from ethynyl glycerol (**6**) to islatravir. We then turned to strategic considerations around how best to integrate these individual reactions into the overall in vitro synthesis. As discussed above, the three reversible reactions catalyzed by PPM, PNP, and SP must take place concurrently to achieve a favorable equilibrium. Extending the simultaneous cascade to include the reversible aldol addition could provide additional synergy. Compatible pH and temperature ranges would allow all four enzymes to function in the same solution. Sucrose phosphorylation as a thermodynamic driving force could pull forward all the equilibria, including the aldol reaction. These factors enabled us to lower the excess of acetaldehyde to levels tolerated by all the enzymes. In this way, we could operate a simultaneous four-enzyme cascade in which the nucleoside degradation pathway runs in reverse, driven to high conversion by phosphate removal (Fig. 2). Islatravir crystallized from the reaction mixture and could be isolated directly through filtration in greater than 95% purity and 76% yield from **5**.

The oxidation and phosphorylation reactions are essentially irreversible, so directly coupling them with the downstream cascade provides no thermodynamic benefit. We considered a tandem GOase-kinase combined reaction, so

that in situ product consumption would minimize the inhibition suffered by the oxidase. Unfortunately, the pantothenate kinase lacked the required chemoselectivity, rapidly phosphorylating triol **6**.

Isolating the intermediates **5** and **7** proved to be challenging because of their high solubility in water. Therefore, we focused on developing a process in which a single aqueous solution was carried through the entire sequence. This approach necessitated evaluating the impact of each component on the remaining steps. The use of acetyl phosphate as the phosphorous donor requires neutralization of the liberated acetic acid, generating a solution with elevated ionic strength. The high salt content inhibits downstream enzymes—in particular, the hexameric PNP (figs. S15 and S16). To enable these reactions to proceed effectively, we carried out further PNP evolution under high-salt conditions and diluted the kinase product solution to reduce its ionic strength before the next step.

With a total of nine enzymes used in the synthesis and no intermediate isolations, management of cumulative protein content was critical. The final filtration of crystallized islatravir became difficult as the amount of protein in the mixture increased. The homogeneous nature of the oxidation and phosphorylation reactions opened the possibility of immobilizing their enzymes to allow easy removal after these steps. For this purpose, we applied an affinity immobilization technique that relies on the capture of polyhistidine-tagged proteins on a metal-containing solid support (27). The recombinant oxidase and kinase enzymes were immobilized in this way, which had the added benefit of eliminating nontagged proteins during immobilization and minimizing

**Table 1. Properties and performance of evolved enzymes used in the biocatalytic pathway.**

Enzyme	Source organism	Evolution focus	Starting enzyme		Evolved variant		
			Rounds of evolution	Global amino acids changed (no.)	Conversion (selectivity)	Loading (%)*	Conversion (selectivity)
Oxidase (GOase)	<i>Fusarium graminearum</i>	Stereoselectivity	12	34	Variant M1: 33%†† (8:92 <i>R:S</i> )	80%†§ (90:10 <i>R:S</i> )	20
		Activity			Variant F2: 8%†† (40:60 <i>R:S</i> )		
PanK	<i>E. coli</i>	Activity	3	10	<1% (5:1 <i>R:S</i> )†¶	>95% (10:1 <i>R:S</i> )†#	10
DERA	<i>S. halifaxensis</i>	Acetaldehyde tolerance	2	11	97%**[>98:1:1 (3S4R): (3R4R):(3S4S)]	97%**[>98:1:1 (3S4R): (3R4R):(3S4S)]	0.2
PPM	<i>E. coli</i>	Activity	2	5	0.5%††	34%††	0.5
PNP	<i>E. coli</i>	Activity	4	7	0.18%†† (>99.5:0.5 <i>dr</i> )	62%†† (>99.5:0.5 <i>dr</i> )	0.125

\*Enzyme loading refers to the mass of lyophilized clarified cell lysate relative to the mass of the reaction substrate. Results may reflect improvements in enzyme expression as well as activity. †Reaction with nonimmobilized enzymes. ‡GOase-M1-Strep and F2-Strep: 172 mM **6**, pH 7.5, 0.2 mM CuSO<sub>4</sub>, 25°C, 4 hours. §GOase-13BB-His: 258 mM **6**, pH 7.5, 0.2 mM CuSO<sub>4</sub>, 25°C, 4 hours. ¶144 mM **7**, pH 7.5, 20°C, 18 hours. #235 mM **7**, pH 6.4, 20°C, 18 hours. \*\*142 mM **5**, 420 mM acetaldehyde, pH 7.2, 30°C, 24 hours. ††15 mM **4**, 5 mM MnCl<sub>2</sub>, pH 7.5, 40°C, 18 hours. †††13 mM **1b**, pH 7.5, 40°C, 16 hours.

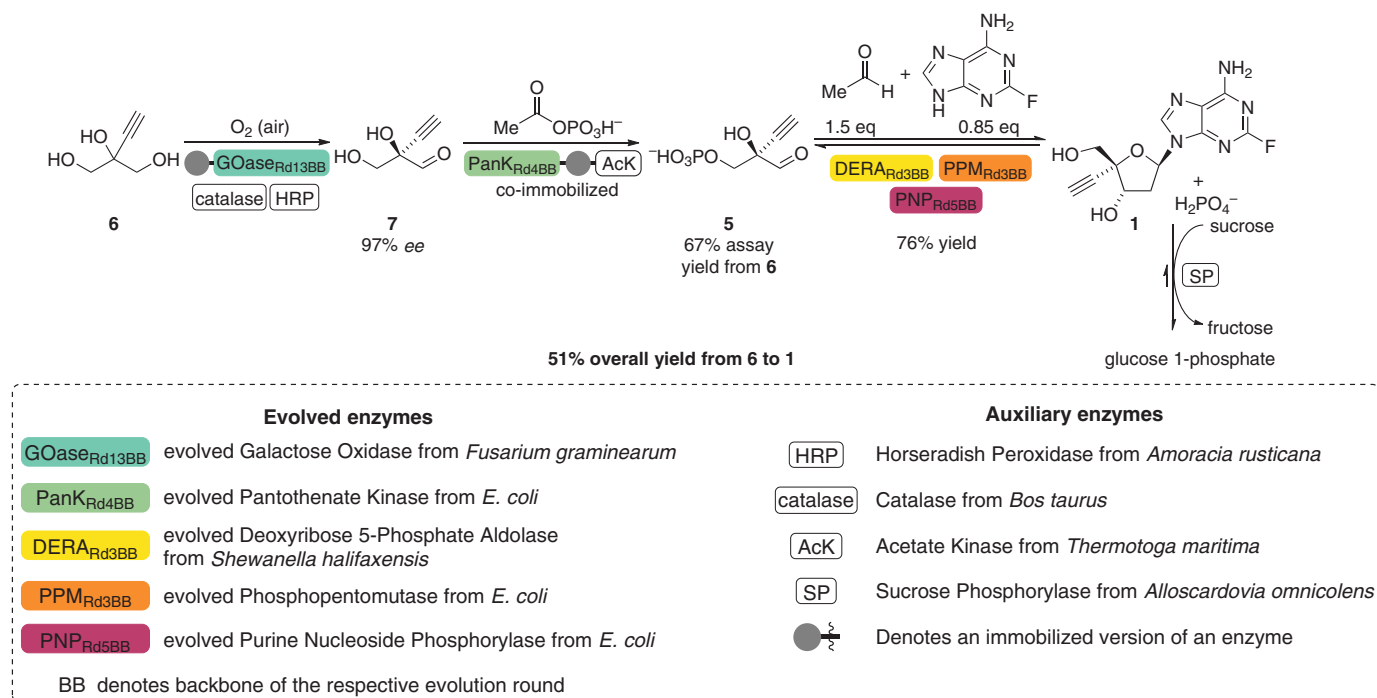


**Fig. 2. Fully assembled biocatalytic pathway.** Evolved enzymes are in colored boxes, and wild-type auxiliary enzymes are in white boxes.

undesired side reactions catalyzed by host-cell enzymes. Immobilization was not pursued for the aldol and glycosylation enzymes because the product crystallizes during this step.

The biocatalytic synthesis produces only a single stereoisomer of islatravir in a self-correcting manner. Oxidative desymmetrization establishes the fully substituted carbon center with 90:10 selectivity, and the ratio is increased by further oxidation of the minor enantiomer. Every subsequent step provides an opportunity to amplify the stereochemical purity. The kinase and aldolase enzymes react with kinetic selectivity toward the (*R*)-aldehydes **7** and **5**, respectively, allowing upgrade of the enantiomer ratio. The aldolase creates the second stereogenic center with great precision. Last, only the (*3S,4R*)-diastereomer of the sugar phosphate **4** can react further, and the glycosylation sets the anomeric center with perfect selectivity.

The full in vitro biocatalytic cascade uses five engineered enzymes and four auxiliary enzymes to stereoselectively assemble islatravir from simple achiral building blocks in 51% overall yield. The atom economy far exceeds that of previous syntheses of this target, and the number of steps is less than half. The entire sequence takes place under mild conditions in a single aqueous solution without the isolation of intermediates. This extraordinary efficiency was made possible by the ability to identify and engineer enzymes that can build complex structures with excellent stereo- and chemoselectivity and without the need for pro-

tecting groups. We envision a growing adoption of cascade biocatalysis as a strategy for the sustainable synthesis of complex non-natural molecules such as pharmaceuticals. The application of enzyme cascades to a diverse range of molecular structures will rely on further advances in the pace of protein engineering (28) and the continuing discovery of new enzymatic transformations (7, 29).

#### REFERENCES AND NOTES

- K. R. Campos *et al.*, *Science* **363**, eaat0805 (2019).
- R. A. Sheldon, J. M. Woodley, *Chem. Rev.* **118**, 801–838 (2018).
- N. J. Turner, L. Humphreys, *Biocatalysis in Organic Synthesis* (The Royal Society of Chemistry, 2018).
- J. H. Schrittwieser, S. Velikogne, M. Hall, W. Kroutil, *Chem. Rev.* **118**, 270–348 (2018).
- S. P. France, L. J. Hepworth, N. J. Turner, S. L. Flitsch, *ACS Catal.* **7**, 710–724 (2017).
- F. H. Arnold, *Q. Rev. Biophys.* **48**, 404–410 (2015).
- F. H. Arnold, *Angew. Chem. Int. Ed.* **57**, 4143–4148 (2018).
- H. Ohruu *et al.*, *Nucleosides Nucleotides Nucleic Acids* **26**, 1543–1546 (2007).
- E. Michailidis *et al.*, *J. Biol. Chem.* **289**, 24533–24548 (2014).
- S. E. Barrett *et al.*, *Antimicrob. Agents Chemother.* **62**, e01058-18 (2018).
- M. McLaughlin *et al.*, *Org. Lett.* **19**, 926–929 (2017).
- M. Kageyama, T. Nagasawa, M. Yoshida, H. Ohruu, S. Kuwahara, *Org. Lett.* **13**, 5264–5266 (2011).
- K. Fukuyama, H. Ohruu, S. Kuwahara, *Org. Lett.* **17**, 828–831 (2015).
- M. Kageyama *et al.*, *Biosci. Biotechnol. Biochem.* **76**, 1219–1225 (2012).
- S. Kohgo, H. Ohruu, M. Matsuoka, H. Mitsuya, 4'-C-substituted-2-haloadenosine derivative, U.S. patent no. US7625877 B2 (2009).
- N. J. Turner, E. O'Reilly, *Nat. Chem. Biol.* **9**, 285–288 (2013).
- I. A. Mikhailopolu, A. I. Miroshnikov, *Acta Naturae* **2**, 36–59 (2010).
- M. G. Tozzi, M. Camici, L. Mascia, F. Sgarrella, P. L. Ipata, *FEBS J.* **273**, 1089–1101 (2006).
- W. R. Birmingham *et al.*, *Nat. Chem. Biol.* **10**, 392–399 (2014).

- C. L. Windle, M. Müller, A. Nelson, A. Berry, *Curr. Opin. Chem. Biol.* **19**, 25–33 (2014).
- K. Hammer-Jespersen, A. Munch-Petersen, *Eur. J. Biochem.* **17**, 397–407 (1970).
- W. Tischer, H.-G. Ihlenfeldt, O. Barzu, H. Sakamoto, E. Pistotnik, P. Marière, S. Pochet, *Enzymatic synthesis of deoxyribonucleosides*, U.S. patent no. US07229797 B1 (2007).
- M. Dick *et al.*, *Chem. Sci.* **7**, 4492–4502 (2016).
- L. Sun, I. P. Petrounia, M. Yagasaki, G. Bandara, F. H. Arnold, *Protein Eng. Des. Sel.* **14**, 699–704 (2001).
- J. B. Rannes *et al.*, *J. Am. Chem. Soc.* **133**, 8436–8439 (2011).
- A. Toftgaard Pedersen *et al.*, *Org. Process Res. Dev.* **19**, 1580–1589 (2015).
- M. P. Thompson *et al.*, *Tetrahedron* **75**, 327–334 (2019).
- M. D. Truppo, *ACS Med. Chem. Lett.* **8**, 476–480 (2017).
- P. N. Devine *et al.*, *Nat. Rev. Chem.* **2**, 409–421 (2018).

#### ACKNOWLEDGMENTS

We acknowledge the help and support of the following people. Merck team: J. McIntosh for providing wild-type acid phosphatase and acetate kinase constructs; R. Cohen, X. Wang, M. Reibarkh, and P. Dormer for nuclear magnetic resonance analysis support; R. Patel, C. Mastyskarz, W. Pan, J. Gouker, I. Farasat, J. Russell, and L. Do for supporting protein engineering and directed evolution workflows; A. Kassim, T. Andreani, and R. Matthew for help with the preparation of synthetic intermediates; and E. Margelefsky, K. Mattern, M. Miller, and H. Rose for reaction optimization support in scale-up experiments. Codexis team: A. Ortega, A. Sowell-Kantz, H. Maniar, J. Slaton, C. Micklitsch, L. Miller, and M. Krawczyk for library screening support; V. Mitchell, C. Selim, and A. Petkova for library construction support; N. Subramanian and N. Dellas for library design support; J. Riggins for analytical development support; J. Vroom and S. Sivaramakrishnan for enzyme characterization support; and D. Entwistle for chemistry support. **Funding:** This work was funded by Merck & Co., Inc. **Author contributions:** M.A.H. and A.F. carried out and supervised chemistry development and prepared the manuscript. K.R.C., P.N.D., K.M.M. and M.D.T. supervised chemistry development. O.A. and K.A.C. supervised enzyme evolution. J.H.F., S.T.G., G.J.H., J.N.K., J.C.M., M.M., C.C.N., N.R.P., S.A.R., A.M.W., Y.X., and H.Y. carried out chemistry development. M.B.-G., D.D., J.L., N.M.M., G.S.M., J.N., and S.N. carried out enzyme evolution. H.M.H., J.J., L.A.J., and B.F.M. developed analytical methods to allow chemistry development

and enzyme evolution. A.R.-G., E.C.S., D.V., and L.X. carried out computational work to support enzyme discovery and evolution.

**Competing interests:** Merck & Co., Inc. has filed a patent application covering the process: U.S. patent application no. PCT/US2019/040316. Codexis, Inc. has filed patent applications covering the evolved enzymes: U.S. patent application nos. PCT/US2019/040353, PCT/US2019/040359, PCT/US2019/040369, PCT/US2019/040376, and PCT/US2019/040379. **Data and**

**materials availability:** All data are available in the main text or the supplementary materials.

#### SUPPLEMENTARY MATERIALS

[science.sciencemag.org/content/366/6470/1255/suppl/DC1](http://science.sciencemag.org/content/366/6470/1255/suppl/DC1)

Materials and Methods

Figs. S1 to S28

Tables S1 to S15

Schemes S1 to S81

DNA and amino acid sequences of the enzymes

NMR Spectra

HR-MS Spectra

References (30–50)

12 August 2019; accepted 24 October 2019

10.1126/science.aay8484

## Design of an in vitro biocatalytic cascade for the manufacture of islatravir

Mark A. Huffman, Anna Fryszkowska, Oscar Alvizo, Margie Borra-Garske, Kevin R. Campos, Keith A. Canada, Paul N. Devine, Da Duan, Jacob H. Forstater, Shane T. Grosser, Holst M. Halsey, Gregory J. Hughes, Junyong Jo, Leo A. Joyce, Joshua N. Kolev, Jack Liang, Kevin M. Maloney, Benjamin F. Mann, Nicholas M. Marshall, Mark McLaughlin, Jeffrey C. Moore, Grant S. Murphy, Christopher C. Nawrat, Jovana Nazor, Scott Novick, Niki R. Patel, Agustina Rodriguez-Granillo, Sandra A. Robaire, Edward C. Sherer, Matthew D. Truppo, Aaron M. Whittaker, Deeptak Verma, Li Xiao, Yingju Xu and Hao Yang

*Science* **366** (6470), 1255-1259.  
DOI: 10.1126/science.aay8484

### Maximal efficiency from enzyme cascades

Enzymes are highly selective catalysts that can be useful for specific transformations in organic synthesis. Huffman *et al.* combined designer enzymes in a multistep cascade reaction (see the Perspective by O'Reilly and Ryan). The approach eliminates purification steps, recycles expensive cofactors, and couples favorable and unfavorable reactions. With the target molecule islatravir, an experimental HIV drug, they optimized five enzymes by directed evolution to be compatible with unnatural substrates and stable in the reaction conditions. Stereochemical purity was amplified at every enzymatic step, and the final synthesis was both atom economical and efficient.

*Science*, this issue p. 1255; see also p. 1199

#### ARTICLE TOOLS

<http://science.sciencemag.org/content/366/6470/1255>

#### SUPPLEMENTARY MATERIALS

<http://science.sciencemag.org/content/suppl/2019/12/04/366.6470.1255.DC1>

#### RELATED CONTENT

<http://science.sciencemag.org/content/sci/366/6470/1199.full>

#### REFERENCES

This article cites 42 articles, 9 of which you can access for free  
<http://science.sciencemag.org/content/366/6470/1255#BIBL>

#### PERMISSIONS

<http://www.sciencemag.org/help/reprints-and-permissions>

Use of this article is subject to the [Terms of Service](#)

---

*Science* (print ISSN 0036-8075; online ISSN 1095-9203) is published by the American Association for the Advancement of Science, 1200 New York Avenue NW, Washington, DC 20005. The title *Science* is a registered trademark of AAAS.

Copyright © 2019 The Authors, some rights reserved; exclusive licensee American Association for the Advancement of Science. No claim to original U.S. Government Works